The Protein Journal
https://doi.org/10.1007/s10930-018-9791-9

Synthesis and Biological Activity of Scyllatoxin-Based BH3 Domain Mimetics Containing Two Disulfide Linkages

Danushka Arachchige[1] · **Justin M. Holub**[1,2,3]

Abstract
The B cell lymphoma 2 (BCL2) proteins are a family of evolutionarily related proteins that act as positive or negative regulators of the intrinsic apoptosis pathway. Overexpression of anti-apoptotic BCL2 proteins in cells is associated with apoptotic resistance, which can result in cancerous phenotypes and pathogenic cell survival. Consequently, anti-apoptotic BCL2 proteins have attracted considerable interest as therapeutic targets. We recently reported the development of a novel class of synthetic protein based on scyllatoxin (ScTx) designed to mimic the helical BH3 interaction domain of the pro-apoptotic BCL2 protein Bax. These studies showed that the number and position of native disulfide linkages contained within the ScTx-Bax structure significantly influences the ability for these constructs to target anti-apoptotic BCL2 proteins in vitro. The goal of the present study is to investigate the contribution of two disulfide linkages in the folding and biological activity of ScTx-Bax proteins. Here, we report the full chemical synthesis of three ScTx-Bax sequence variants, each presenting two native disulfide linkages at different positions within the folded structure. It was observed that two disulfide linkages were sufficient to fold ScTx-Bax proteins into native-like architectures reminiscent of wild-type ScTx. Furthermore, we show that select (bis)disulfide ScTx-Bax variants can target Bcl-2 (proper) in vitro and that the position of the disulfide bonds significantly influences binding affinity. Despite exhibiting only modest binding to Bcl-2, the successful synthesis of ScTx-Bax proteins containing two disulfide linkages represents a viable route to ScTx-based BH3 domain mimetics that preserve native-like conformations. Finally, structural models of ScTx-Bax proteins in complex with Bcl-2 indicate that these helical mimetics bind in similar configurations as wild-type Bax BH3 domains. Taken together, these results suggest that ScTx-Bax proteins may serve as potent lead compounds that expand the repertoire of "druggable" protein–protein interactions.

Keywords Miniature protein · Scyllatoxin · BH3 domain mimetic · Anti-apoptotic BCL2 protein · Disulfide linkage · Orthogonal protecting group

1 Introduction

Peptides and small proteins that fold into stable three-dimensional structures have emerged as highly potent inhibitors of protein–protein interactions (PPIs) [1–4]. In general, the large, shallow contact area of PPIs makes them difficult or impossible to target using small molecules. As a consequence, stabilized peptides and small proteins that contain elements of secondary or tertiary structure are being developed as ligands to inhibit PPIs with high specificity [5–7]. Miniature proteins represent a class of small, well-folded oligopeptides that adopt stable tertiary structures in solution. Despite their relatively short sequence lengths, miniature proteins are able to fold into protein-like architectures that contain defined helices, sheets, loops and turns. A working hypothesis is that miniature proteins can be developed as

Electronic supplementary material The online version of this article (https://doi.org/10.1007/s10930-018-9791-9) contains supplementary material, which is available to authorized users.

✉ Justin M. Holub
holub@ohio.edu

[1] Department of Chemistry and Biochemistry, Ohio University, Biochemistry Research Facility 108, 350 W. State St., Athens, OH 45701, USA

[2] Molecular and Cellular Biology Program, Ohio University, Athens, OH 45701, USA

[3] Edison Biotechnology Institute, Ohio University, Athens, OH 45701, USA

Published online: 20 August 2018

mimetics of discrete protein interaction domains by grafting specific epitopes to analogous structural elements of the miniature protein scaffold [2, 6, 8]. Due to their biomimetic nature and synthetic tractability, miniature proteins have been used extensively as chemical genetics agents to study and inhibit myriad biomolecular interactions [9–13].

Proteins in the BCL2 family are central regulators of intrinsic apoptosis, a form of active cell suicide induced during times of prolonged cellular stress [14–16]. Currently, there are 25 known genes in the BCL2 family, each of which has either pro- or anti-apoptotic function [17]. Proteins in the BCL2 family are characterized by four conserved BCL2 homology domains (BH1-4) that are crucial for biological function [18, 19]. More specifically, BCL2 proteins are categorized into three subclasses: (1) anti-apoptotic, (2) pro-apoptotic and (3) BH3-only [16]. Pro-apoptotic BCL2 proteins, such as Bax and Bak, mediate apoptosis by controlling the release of apoptogenic factors from the mitochondrial matrix. Anti-apoptotic BLC2 proteins, such as Bcl-2 (proper), Bcl-X_L and Mcl-1, bind and sequester pro-apoptotic BCL2 proteins on the surface of the mitochondria, preventing the release of cytochrome C [15]. Pro-apoptotic BCL2 proteins interact with anti-apoptotic members *via* helical BH3 domains that target shallow, hydrophobic binding clefts on the surface of anti-apoptotic BCL2 proteins [20]. BH3-only proteins, such as Bim, Bad and Noxa are upregulated during times of cellular stress and convey pro-death signals by disrupting the interaction between pro- and anti-apoptotic BCL2 members [17–19, 21]. Anti-apoptotic BCL2 proteins are implicated in pathogenic cell survival and the overexpression of certain BCL2 family members has been linked to disease progression including cancer and autoimmunity [21, 22]. Consequently, anti-apoptotic BCL2 proteins are now considered important therapeutic targets. Despite intense effort however, the ability to selectively target and inhibit discrete members of the BCL2 family has met with only moderate success [23, 24]. Indeed, high degrees of sequence homology and non-selective hydrophobic interactions has made targeting select BCL2:BH3 interactions a significant challenge. Nevertheless, several potent small molecule and stabilized α-helical peptide inhibitors of this interaction have been developed [5, 25, 26]. The BCL2:BH3 interaction is therefore considered an ideal model system with which to test the efficacy of novel ligands that probe the fundamental nature of PPIs.

We recently developed a series of helical BH3-domain mimetics based on the small protein scyllatoxin (ScTx) [27, 28]. ScTx is a 31-amino acid protein isolated from scorpion venom that folds into an α/β structural motif stabilized by three disulfide linkages between cysteines C3–C21, C8–C26 and C12–C28 [29]. Miniature proteins, such as ScTx possess many desirable attributes that potentiate their development as ligands to target PPIs. For example, their small size makes them synthetically tractable, allowing for a high-level of control over the primary sequence. Furthermore, the ScTx protein fold contains an α-helix and β-sheet, each of which can be re-engineered to display functional epitopes for enhanced biomolecular recognition [6, 11]. Our previous work involved grafting residues of the Bax BH3 domain important for BCL2 recognition to the α-helix of ScTx [27, 28]. These constructs were then used as tools to better understand the molecular nature of BCL2:BH3 interactions by targeting anti-apoptotic BCL2 proteins in vitro. It was demonstrated that ScTx-Bax BH3 domain mimetics containing three native disulfides did not bind Bcl-2, while ScTx-Bax proteins containing no disulfide linkages targeted Bcl-2 with nanomolar affinity [27]. These results suggested that an induced-fit binding mechanism is required for favorable BCL2:BH3 interactions. We subsequently developed a series of ScTx-Bax BH3 domain mimetics that contained a single native disulfide linkage at varying positions within the miniature protein sequence [28]. These studies showed that the position of the disulfide significantly influenced the ability for ScTx-Bax proteins to target Bcl-2 in vitro. Specifically, it was found that positioning the disulfide linkage near the middle or C-terminus of the ScTx-Bax BH3 domain (C8–C26 or C12–C28) resulted in favorable targeting of Bcl-2. Alternatively, positioning the disulfide linkage near the N-terminus of the ScTx-Bax BH3 domain (C3–C21) completely abolished binding. These results indicated that greater flexibility near the N-terminus of the BH3 helix may be required for favorable BCL2:BH3 interactions.

We now seek to determine the influence of two disulfide linkages on the folding and biological activity of ScTx-Bax BH3 domain mimetics. To address this issue, we synthesized three ScTx-Bax sequence variants that contain two native disulfide linkages at varying positions within the ScTx-Bax protein. Because wild-type ScTx contains three native disulfide linkages, the ScTx-Bax sequence variants developed in this study contain all possible combinations of native (bis)disulfide patterning. Importantly, this report outlines a successful synthetic route to ScTx-based BH3 domain mimetics that contain two disulfide bonds. Therefore, the de novo design and synthesis of ScTx-based BH3 domain mimetics containing any combination of native disulfides is now possible. Moreover, these studies further establish ScTx-Bax BH3 domain mimetics as potential modulators of Bcl-2 function.

2 Materials and Methods

2.1 Reagents and Chemicals

All Fmoc-protected amino acids, Fmoc-PAL-AM resin and coupling reagents used for peptide synthesis were purchased

from Novabiochem (Billerica, MA). Fmoc-Cys(Acm)-OH was obtained from Bachem (Torrance, CA). *N,N*-Diisopropylethylamine (DIEA), *N*-methyl-2-pyrrolidone (NMP), piperidine, isopropyl β-D-1-thiogalactopyranoside (IPTG), trypsin, ammonium persulfate, iodine and triisopropylsilane (TIPS) were obtained from Sigma-Aldrich (St. Louis, MO). 5-Carboxyfluorescein (5-CF) and dimethyl sulfoxide (DMSO) were obtained from Santa Cruz Biotechnology (Dallas, TX). Acetonitrile (ACN) and D-(+)-glucose were purchased from Alfa Aesar (Ward Hill, MA). Ethylenediaminetetraacetic acid (EDTA) and monobasic sodium phosphate were purchased from Fisher Scientific (Pittsburg, PA). Tris (base), bisacrylamide, sodium dodecyl sulfate (SDS), tetramethylethylenediamine (TEMED), methanol, glacial acetic acid, phenol, imidazole, LB agar, sodium chloride, ampicillin, bacterial protein extraction reagent (B-PER) and protease inhibitors were purchased from Thermo Fisher Scientific (Waltham, MA). Protein marker was obtained from New England Biolabs (Ipswitch, MA). Ni–NTA agarose resin was purchased from Molecular Cloning Laboratories (San Francisco, CA). LB Medium was obtained from MP Biomedicals (Santa Ana, CA). Unless otherwise stated, all other reagents were obtained from commercial sources and used without further purification.

2.2 Solid-Phase Peptide Synthesis

All peptides and miniature proteins described herein were synthesized on Fmoc-PAL-AM resin using standard Fmoc-based synthesis protocols [30]. Oligopeptides were synthesized on a 25 µmol scale that was based on the resin loading level. Amino acid couplings and deprotection reactions were performed in a microwave-accelerated reaction system (CEM, Matthews, NC) using software programs written in-house. To facilitate synthesis, the resin was washed 3 × with NMP following each coupling and deprotection step. Amide bond formations were achieved by treating the resin with 5 equivalents (eq) of amino acid, 5 eq of PyClock and 10 eq of DIEA in NMP. All equivalents were based on the resin loading level. N-terminal Fmoc groups were removed by treating the resin with 25% (v/v) piperidine in NMP containing 0.15 M HOBt to minimize aspartimide formation [31]. Iterative cycles of amino acid coupling and deprotection were performed until oligopeptides of desired sequence were generated. Following synthesis, resin-bound peptides were labeled at the N-terminus with 5-CF. To facilitate labeling, 5-CF was pre-activated by dissolving 5 eq of 5-CF in NMP containing 5 eq HCTU (Peptides International, Louisville, KY) and 10 eq DIEA. This mixture was allowed to stir in the dark for 20 min. Following activation, the labeling solution was added to the resin-bound peptide and the reaction was allowed to stir in the dark for 24 h at room temperature. Once completed, the resin was washed 5 × with NMP, 5 × with alternating volumes of NMP and dichloromethane, and 5 × with dichloromethane. The resin was then allowed to dry under vacuum in the dark for 6 h at room temperature to remove residual solvent.

2.3 Cleavage and Purification

Resin-bound peptides were globally deprotected and cleaved from the solid-support by treating the resin with cleavage cocktail (88:5:5:2, v/v/v/v, TFA:water:phenol:TIPS). This reaction mixture was added to the resin and allowed to incubate for 30 min at 38 °C in a microwave reactor (CEM). Following cleavage, the peptides were precipitated in cold diethyl ether, pelleted by centrifugation and re-suspended in 15% (v/v) ACN in water. This mixture was then frozen and lyophilized to dryness; all peptide powders were stored under nitrogen prior to purification to minimize potential air oxidation. Following lyophilization, crude peptide powders were re-suspended in a suitable volume of 10% (v/v) ACN in water to a final concentration of approximately 15 mg mL^{-1} and purified across a semi-preparatory scale reversed-phase C18 column (Grace, 10 µm, 250 × 10 mm I.D.) using an ProStar HPLC system (Agilent). For each purification, 5–10 mg peptide was loaded onto the column and eluted over 30 min with a linear AB gradient of 15–45% (1% ACN min^{-1}), where A is 0.1% TFA in water and B is 0.1% TFA in ACN. Absorbance spectra were monitored at 214 nm and 450 nm to distinguish between labeled and unlabeled peptide products. The identities of the eluted peptides were determined using mass spectrometry (*vide infra*). Product peaks were collected, combined, frozen and lyophilized to dryness before being subjected to subsequent oxidation (folding) reactions. For control peptides not being subjected to subsequent oxidation, purified powders were reconstituted in water and stored at 4 °C protected from light. The concentrations of stock peptide solutions were quantified using an extinction coefficient for 5-CF of 83,000 M^{-1} cm^{-1} at 450 nm in water (Setareh Biotech, Eugene, OR).

2.4 Oxidative Folding

Oxidative folding of reduced ScTx-Bax BH3 domain mimetics was performed using modifications of methods described previously [32]. To form the first disulfide linkage, linear peptides containing two free thiols were dissolved in 50% (v/v) ACN in water at a final concentration of 0.02 mg mL^{-1}. Once the peptides were dissolved, DMSO was added to the solution at a final concentration of 20% (v/v) and the pH was adjusted to 6.0 with 1 M HCl. The reaction was then stirred for 24 h at room temperature in the dark. Once completed, the reaction was quenched with the addition of TFA at a final concentration of 5% (v/v) and the mixture was purified across a semi-preparatory scale reversed-phase C18 column

(Grace, 10 µm, 250 × 10 mm I.D.) using an ProStar HPLC system (Agilent). Semi-reduced peptides containing one disulfide linkage were eluted over 30 min with a linear AB gradient of 15–45% (1% ACN min^{-1}). Absorbance spectra were monitored at 214 nm to distinguish between fully- and semi-reduced products. The identities of the eluted peptides were evaluated by mass spectrometry and oxidized products were confirmed by a loss in mass corresponding to two hydrogen atoms. Product peaks containing oxidized peptides were collected, combined, frozen and lyophilized to dryness before being subjected to subsequent oxidation reactions.

To form the second disulfide linkage, semi-oxidized peptides containing Acm-protected cysteines were dissolved in a solution of glacial acetic acid and 0.1 M HCl (4:1, v/v) at a final concentration of 0.02 mg mL^{-1}. Once the peptides were dissolved, 50 eq iodine (0.05 M in MeOH) were added to the solution and the mixture was stirred at room temperature for 2 h in the dark. The fully-oxidized proteins were then purified across a reversed-phase C18 column (Grace, 10 µm, 250 × 10 mm I.D.) using an ProStar HPLC system (Agilent). Peptides containing two disulfide linkages were eluted over 30 min with a linear AB gradient of 15–45% (1% ACN min^{-1}). Absorbance spectra were monitored at 214 nm to distinguish between fully- and semi-oxidized products. The identities of the eluted proteins were evaluated by mass spectrometry and fully-oxidized products were confirmed by observing a loss in mass corresponding to two hydrogen atoms. Product peaks containing fully-oxidized ScTx-Bax proteins were collected, combined, frozen and lyophilized twice. Product powders were reconstituted in water and stored at 4 °C protected from light. The concentrations of stock solutions were quantified using an extinction coefficient for 5-CF of 83,000 M^{-1} cm^{-1} at 450 nm in water (Setareh Biotech, Eugene, OR).

2.5 General Characterization by ESI-MS and Analytical HPLC

The identities of all synthetic peptides and miniature proteins described herein were confirmed using electrospray ionization mass spectrometry (ESI-MS). Product masses were determined using a Thermo Scientific Q Exactive Plus Hybrid Quadrupole-Orbitrap Mass Spectrometer in the m/z range of 500–2200. For analysis, products were dissolved in 500 µL water and directly injected at a flow rate of 10 µL min^{-1}. All mass data were processed using Xcalibur v3.0 (Thermo) and MagTran v1.0 deconvolution software (Amgen, Thousand Oaks, CA). Product purities were evaluated by analytical reversed-phase HPLC using an Agilent ProStar system. Compounds (2.5 µM in water) were analyzed across an analytical scale reversed-phase C18 column (Grace, 5 µm, 50 × 2.1 mm I.D.) and eluted over 20 min with a linear AB gradient of 5–95% (4.5% ACN min^{-1}). All products were purified to > 95% as determined by product peak integration of analytical HPLC chromatograms. Analytical HPLC data were processed using OpenLab CDS ChemStation Software (Agilent) v1.06 and KaleidaGraph v4.5 (Synergy Software).

2.6 Disulfide Bridge Assignment

To confirm the correct position of the disulfide linkages, oxidized ScTx-Bax proteins were mixed with trypsin (10% w/v) at a final concentration of 0.1 µg $µL^{-1}$ in 100 µL digestion buffer (100 mM Tris, 1 mM $CaCl_2$, pH 7.8) and allowed to incubate at 37 °C for 2 h. Once the reactions were complete, 100 µL of 50% (v/v) TFA in water was added to stop proteolysis. The entire reaction mixture was then loaded onto an analytical scale C18 reversed-phase HPLC column (Grace, 5 µm, 50 × 2.1 mm I.D.) and digested products were eluted over 50 min with a linear AB gradient of 0–50% (1% ACN min^{-1}) at a flow rate of 1 mL min^{-1}. Product peaks were collected and analyzed by mass spectrometry. As a negative control, proteases were similarly incubated in digestion buffer without protein for 2 h at 37 °C to verify that there were no autolytic fragments present in the reaction.

2.7 Structural Characterization

The solution-phase structures of fully-oxidized ScTx-Bax BH3 domain mimetics were evaluated by wavelength-dependent circular dichroism (CD) spectroscopy. For analysis, stock solutions of ^{Flu}ScTx-Bax$^{\Delta}$ proteins were diluted to a final concentration of 5 µM in binding buffer (50 mM Tris, 100 mM NaCl, pH 8.0). All test solutions were allowed to incubate at 20 °C for 10 min before being analyzed by CD spectroscopy. Wavelength scans were performed on a Jasco J-715 spectropolarimeter at 20 °C. Each spectrum represents a background subtracted (buffer only) average of three scans. Data were processed with J-700 Software v1.5 (Jasco) and KaleidaGraph v4.5 (Synergy Software).

2.8 Protein Expression and Purification

His-tagged Bcl-2-ΔTM proteins were expressed from BL21(DE3) competent cells using a modification of methods described previously [27, 33]. Briefly, bacterial cells harboring Bcl-2 plasmids were grown as 1 L cultures in LB media containing 100 µg mL^{-1} ampicillin to an optimized OD_{600} of 0.8 at 37 °C. Protein expression was induced for 4 h at 37 °C with the addition IPTG at a final concentration of 1 mM. Following induction, the bacteria were pelleted and stored at − 80 °C until further use. To extract the expressed protein, bacterial pellets were re-suspended in 10 mL cold B-PER including 10 mM imidazole and EDTA-free protease inhibitor tablets (Thermo Fisher, #A32955) containing aprotinin,

bestatin, E-64, leupeptin, 4-(2-aminoethyl)benzenesulfonyl fluoride (AEBSF) and pepstatin. This suspension was then allowed to shake at 4 °C for 10 min before being centrifuged at 15,000 × *g* for 15 min at 4 °C. The cleared lysate was then added across a freshly prepared Ni–NTA agarose column according to the manufacturer's instructions. The protein was eluted from the column with elution buffer (50 mM NaH_2PO_4, 500 mM NaCl, 250 mM imidazole, pH 8.0) and dialyzed into binding buffer (50 mM Tris, 100 mM NaCl, pH 8.0). To determine purity of the eluted protein, samples of the collected fractions were loaded onto a 10% polyacrylamide gel and separated by SDS–PAGE. Visualization of the proteins was achieved by staining the gel with Coomassie Blue (data not shown). Following dialysis, the protein was concentrated using centrifugal filtration units (Millipore) to a final concentration of 15 µM. Concentrated protein solutions were aliquoted, flash frozen and stored at − 80 °C until further use.

2.9 Fluorescence Polarization

All fluorescence polarization (FP) binding experiments were performed using methods described previously [28, 34]. For these studies, serial dilutions of Bcl-2-ΔTM were prepared in binding buffer on black 384-well plates (#3575, Corning, Corning, NY) and an aliquot of fluorescently-labeled peptide or protein was added to each dilution at a final concentration of 25 nM. The plates were sealed using aluminum sealing tape (#6569, Corning, Corning, NY) and the reactions were allowed to incubate in the dark at 25 °C for 1 h. This incubation time was sufficient for binding reactions to reach equilibrium, as judged by an absence of significant change in the observed polarization value of the sample with the lowest protein concentration over 4 h. Fluorescence polarization was measured using a SpectraMax M5e multi-mode plate reader (Molecular Devices, Sunnyvale, CA), with an excitation wavelength of 498 nm and an emission wavelength of 525 nm set to an automatic cutoff of 515 nm. An average of 100 reads were recorded for each well. Polarization data were processed using SoftmaxPro v6.4 (Molecular Devices) and binding curves were fit using KaleidaGraph v4.5 to a single-site binding model described by the equation outlined below.

$$FP_{obs} = FP_0 + (FP_{max} - FP_0) \times \frac{1}{2L} \times \left\{ (Kd + P + L) - \sqrt{(Kd + P + L)^2 - (4 \times P \times L)} \right\}$$

where FP_{obs} is the fluorescence polarization at protein concentration *P;* FP_0 is the fluorescence polarization of ligand in the absence of protein ($P = 0$); FP_{max} is the maximum fluorescence polarization at saturation of protein with ligand. *P* and *L* represent the total respective concentrations of protein and ligand, and *Kd* is the dissociation constant.

2.10 Molecular Modeling

All molecules were rendered and aligned using a modified version of the PyMOL Molecular Graphics System v1.8.2, Schrödinger, LLC (PyMOLX11Hybrid). Initially, a model ScTx-Bax protein was prepared for analysis by mutating all appropriate residues of wild-type ScTx (PDB ID: 1SCY) [29] to amino acids corresponding to the N-terminal region of the Bax BH3 domain (residues 54–70). Structural alignments were then performed using a published structure of the Bax BH3 domain in complex with Bcl-2 (PDB ID: 2XA0) [35]. Specifically, residues 5–15 of the ScTx-Bax protein were aligned with residues 58–68 of the Bax BH3 domain in complex with Bcl-2. Following alignment, backbone and sidechain bonds of the ScTx-Bax α-helix were observed to ensure that all torsional angles were within permissible range [36]. Furthermore, the solvent-accessible surfaces of ScTx-Bax and Bcl-2 were assessed to verify that no steric overlap occurred between the complexed proteins.

3 Results

3.1 Rational Design of ScTx-Bax$^{\Delta}$ Proteins

We recently employed a strategy known as protein grafting to develop a series of ScTx-based Bax BH3 domain mimetics that target anti-apoptotic BCL2 proteins in vitro [27, 28]. This technique involved installing residues from the helical Bax BH3 domain important for BCL2 recognition to the α-helix of ScTx (Fig. 1a). Results from our previous studies showed that the number and position of native disulfide linkages within the ScTx-Bax protein play important roles in their folding and biological activity. For example, fully-oxidized ScTx-Bax BH3 domain mimetics containing three native disulfides did not bind Bcl-2 in vitro, while fully-reduced ScTx-Bax variants targeted Bcl-2 with nanomolar affinity. Furthermore, it was demonstrated that the position of single disulfide linkages within the ScTx-Bax sequence significantly affected the ability for these constructs to fold and target Bcl-2 in vitro. In the current study, we sought to determine how the presence of two disulfide linkages influences the folding and biological activity of ScTx-based Bax BH3 domain mimetics. To accomplish this, we designed three ScTx-Bax sequence variants, each containing two native disulfide linkages at varying positions within their primary structures. To facilitate binding to anti-apoptotic BCL2 proteins in vitro, several possible ScTx-Bax sequences were aligned with residues 54–74 of the Bax BH3 domain and

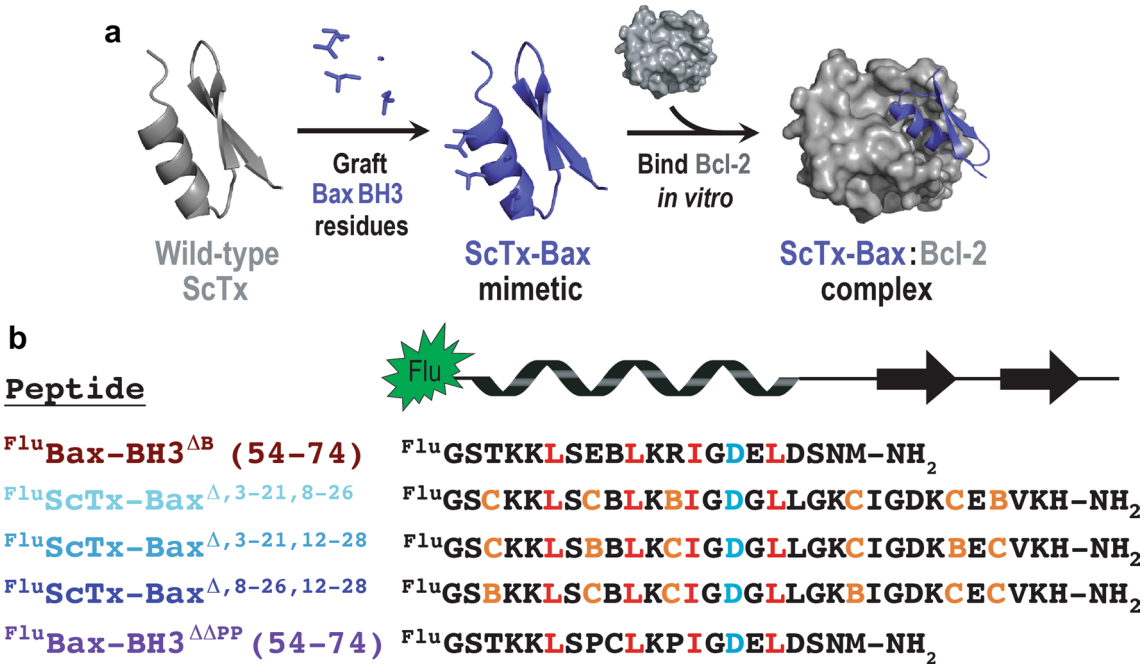

Fig. 1 **a** Protein grafting strategy for targeting anti-apoptotic Bcl-2 proteins with ScTx-based BH3 domain mimetics. Bax BH3 domain residues important for Bcl-2 recognition are grafted onto the α-helix of ScTx. ScTx-Bax proteins are then used to target anti-apoptotic Bcl-2 proteins in vitro. **b** Sequence alignment of fluorescently-labeled Bax BH3 domain peptides and ScTx-Bax$^{\Delta}$ variants used in this work. Key BH3 domain residues involved in Bcl-2 recognition are colored red; aminobutyric acids (B) and cysteines involved in ScTx folding are colored orange; the conserved Bax BH3 domain aspartic acid (D68) is cyan. (Color figure online)

scored based on two primary criteria: (1) the ability to display the functional Bax BH3 epitope (L59, L63, I66, L70) on the solvent-exposed surface of the ScTx α-helix and (2) alignment of ScTx structural cysteines with Bax BH3 residues that point away from the BCL2:BH3 binding interface [35]. This design strategy produced ScTx-Bax proteins that were near identical sequence mimetics of the Bax BH3 domain (Fig. 1b). Structural cysteine residues were judiciously placed within each ScTx-Bax sequence to facilitate the formation of native disulfide linkages between C3–C21, C8–C26 or C12–C28. These sequence mimetics were designated ^{Flu}ScTx-Bax$^{\Delta}$ to signify the removal of one disulfide linkage and labeling of the N-terminus with 5-CF. Furthermore, the numerical position of each disulfide linkage was included in the final nomenclature of each mimetic. For example, fluorescently-labeled ScTx-Bax proteins that contain disulfide linkages between residues C3–C21 and C8–C26 were named ^{Flu}ScTx-Bax$^{\Delta,3-21,8-26}$. To preclude unwanted disulfide formation, additional cysteines within the ScTx-Bax sequences were mutated to aminobutyric acid (Abu, B), which acts as a structural isostere of cysteine [37].

We also designed two BH3 domain peptides, ^{Flu}Bax-BH3$^{\Delta B}$ and ^{Flu}Bax-BH3$^{\Delta\Delta PP}$, to serve as respective positive and negative controls for targeting Bcl-2 in vitro (Fig. 1b). ^{Flu}Bax-BH3$^{\Delta B}$ is a peptide derived from the BH3 domain of Bax (residues 54–74). To mitigate potential oxidation, ^{Flu}Bax-BH3$^{\Delta B}$ includes an Abu residue in place of a cysteine corresponding to C62 of the wild-type Bax sequence. It should be noted that C62 is not known to be directly involved in the BCL2:BH3 interaction [35, 38] and it has been shown that ^{Flu}Bax-BH3$^{\Delta B}$ binds Bcl-2 in vitro with similar affinity compared to wild-type Bax BH3 peptides [28]. As a negative control, we synthesized ^{Flu}Bax-BH3$^{\Delta\Delta PP}$, which contains two prolines that replace residues E61 and R65 in the native Bax-BH3 sequence (Fig. 1b). Proline substitutions have been shown to perturb the ability for linear peptides to form helices in solution [39]; previous studies by our laboratory have demonstrated that ^{Flu}Bax-BH3$^{\Delta\Delta PP}$ has limited helical propensity and is unable to target anti-apoptotic BCL2 proteins in vitro [27, 28].

3.2 Synthesis and Oxidative Folding

All peptides and miniature proteins described herein were manually synthesized on PAL-AM resin using standard Fmoc-based solid-phase peptide synthesis (SPPS) procedures [30]. To facilitate FP direct binding experiments, all constructs were labeled at their N-terminus with 5-CF (see

"Materials and Methods" section). Following cleavage from the resin, HPLC analysis revealed that the SPPS procedure outlined herein yielded a single major product for each respective peptide (data not shown). All ^{Flu}ScTx-Bax$^{\Delta}$ variants were initially purified by reversed-phase HPLC before being subjected to subsequent oxidation reactions. Masses of all purified products were confirmed by electrospray ionization mass spectrometry (Table S1).

Our previous work has shown that disulfide linkages between cysteines C3–C21, C8–C26 and C12–C28 can be formed simultaneously in ScTx-Bax proteins by oxidizing the fully-reduced peptides with glutathione [27]. We therefore attempted a similar strategy to oxidize the two disulfides of ^{Flu}ScTx-Bax$^{\Delta}$ variants. To accomplish this, we synthesized three ^{Flu}ScTx-Bax$^{\Delta}$ peptides that included four cysteines protected with acid-labile trityl (Trt) groups. This synthetic strategy afforded peptides that contained four deprotected thiols following cleavage from the resin. These peptides were then purified by HPLC and reacted in folding buffer containing glutathione as described previously [27, 37]. Unfortunately, this strategy to simultaneously oxidize the two disulfide bonds using glutathione failed. These reactions resulted in heterogeneous mixtures of products that contained native and non-native disulfide linkages. All disulfide linkage patterns were identified using mass spectrometry on trypsin digested products (data not shown). It should be noted that the positions of the cysteines within the primary sequence influenced the extent of disulfide shuffling among ^{Flu}ScTx-Bax$^{\Delta}$ variants when reacted under these conditions. Specifically, the major oxidized product of ^{Flu}ScTx-Bax$^{\Delta,3-21,8-26}$ was found to contain disulfide linkages between C3–C8 and C21–C26, indicating inefficient oxidation between native cysteine residues. Attempting to fold ^{Flu}ScTx-Bax$^{\Delta,3-21,12-28}$ using glutathione did result in the formation of the properly folded product, however this was a minor species (< 25%) in the reaction mixture. The major product in this reaction was found to contain disulfide linkages between cysteines C3–C28 and C12–C21, indicating that glutathione was not efficient at forming disulfides between native cysteine residues in ^{Flu}ScTx-Bax$^{\Delta,3-21,12-28}$ proteins under these conditions. We also attempted to fold fully-reduced ^{Flu}ScTx-Bax$^{\Delta}$ mimetics using a stronger and more selective oxidizing agent: bis(ethylenediamine) platinum(II) chloride ($[Pt(en)_2Cl_2]^{+2}$) [40, 41]. This oxidizing agent has been useful to form intramolecular disulfide linkages in peptides up to 13 amino acids in length [41], and has been used by our laboratory to synthesize ScTx-Bax variants that contain single disulfide bonds [28]. Unfortunately, this approach also proved unsuccessful for the simultaneous oxidation of two native disulfides in ^{Flu}ScTx-Bax$^{\Delta}$ proteins, and resulted in heterogeneous mixtures of products containing native and non-native disulfide linkages (data not shown).

Following these failed attempts, we moved to synthesize fully-oxidized ^{Flu}ScTx-Bax$^{\Delta}$ proteins using orthogonal protecting groups on select cysteine residues and two rounds of sequential oxidation (Fig. 2). Similar approaches have been used previously in the total chemical synthesis of small proteins that contain multiple disulfide linkages [32]. For these studies, we synthesized ^{Flu}ScTx-Bax$^{\Delta}$ variants as described above and installed cysteines that were protected by an acetamidomethyl (Acm) protecting group. This functionality is stable under standard acidic conditions used to cleave peptides from solid support and provides protection for cysteine thiols under oxidative conditions [42]. Following synthesis and cleavage of the reduced peptide, the Acm group can be removed by treating the protected peptides with iodine under mild conditions [43]. To begin, peptides were synthesized using standard SPPS methods as described (see "Materials and Methods" section). To facilitate disulfide formation, we installed Fmoc-Cys(Trt)-OH amino acids at positions that would result in the first disulfide linkage being formed closest to the C-terminus of the helical BH3 domain. For example, ^{Flu}ScTx-Bax$^{\Delta,3-21,8-26}$ had Fmoc-Cys(Trt)-OH amino acids installed at positions C8 and C26, while ^{Flu}ScTx-Bax$^{\Delta,3-21,12-28}$ and ^{Flu}ScTx-Bax$^{\Delta,8-26,12-28}$ had Fmoc-Cys(Trt)-OH amino acids installed at positions C12 and C28. Once synthesized, the peptides were cleaved from the resin as described and the crude products were purified by HPLC. Following purification, the peptides were oxidized by suspending them at a final concentration of 0.2 mg mL^{-1} in aqueous acetonitrile (50% in water) containing 20% DMSO at pH 6.0 and allowing them to stir for 24 h at room temperature in the dark. This reaction afforded semi-oxidized peptide products that contained a native disulfide linkage between deprotected cysteine thiols (Fig. 2). Following the reaction, semi-oxidized peptides were purified by semi-preparative HPLC before subsequent oxidation reactions (Fig. 3a). Importantly, this purification step allowed us to quantify the conversion percentage from fully-reduced to semi-oxidized product. It was observed from this series of reactions that the position of the cysteines significantly influenced the efficacy of the DMSO oxidation. For instance, ^{Flu}ScTx-Bax$^{\Delta,8(Acm),26(Acm),12-28}$ peptides showed the lowest conversion percentage, with the formation of 45.5% oxidized product. The conversion percentage for ^{Flu}ScTx-Bax$^{\Delta,3(Acm),21(Acm),12-28}$ increases to 60.6% under similar conditions, while ^{Flu}ScTx-Bax$^{\Delta,3(Acm),21(Acm),8-26}$ peptides showed the highest conversion at 78.3%. All conversion percentages of fully-oxidized peptides were determined by product peak integration of semi-preparatory HPLC chromatograms (Fig. 3a). These results would suggest that disulfides formed more easily in peptides that had greater distance between the Acm groups and the initial oxidation site (compare conversion percentages for ^{Flu}ScTx-Bax$^{\Delta,8(Acm),26(Acm),12-28}$ and ^{Flu}ScTx-Bax$^{\Delta,3(Acm),21(Acm),12-28}$).

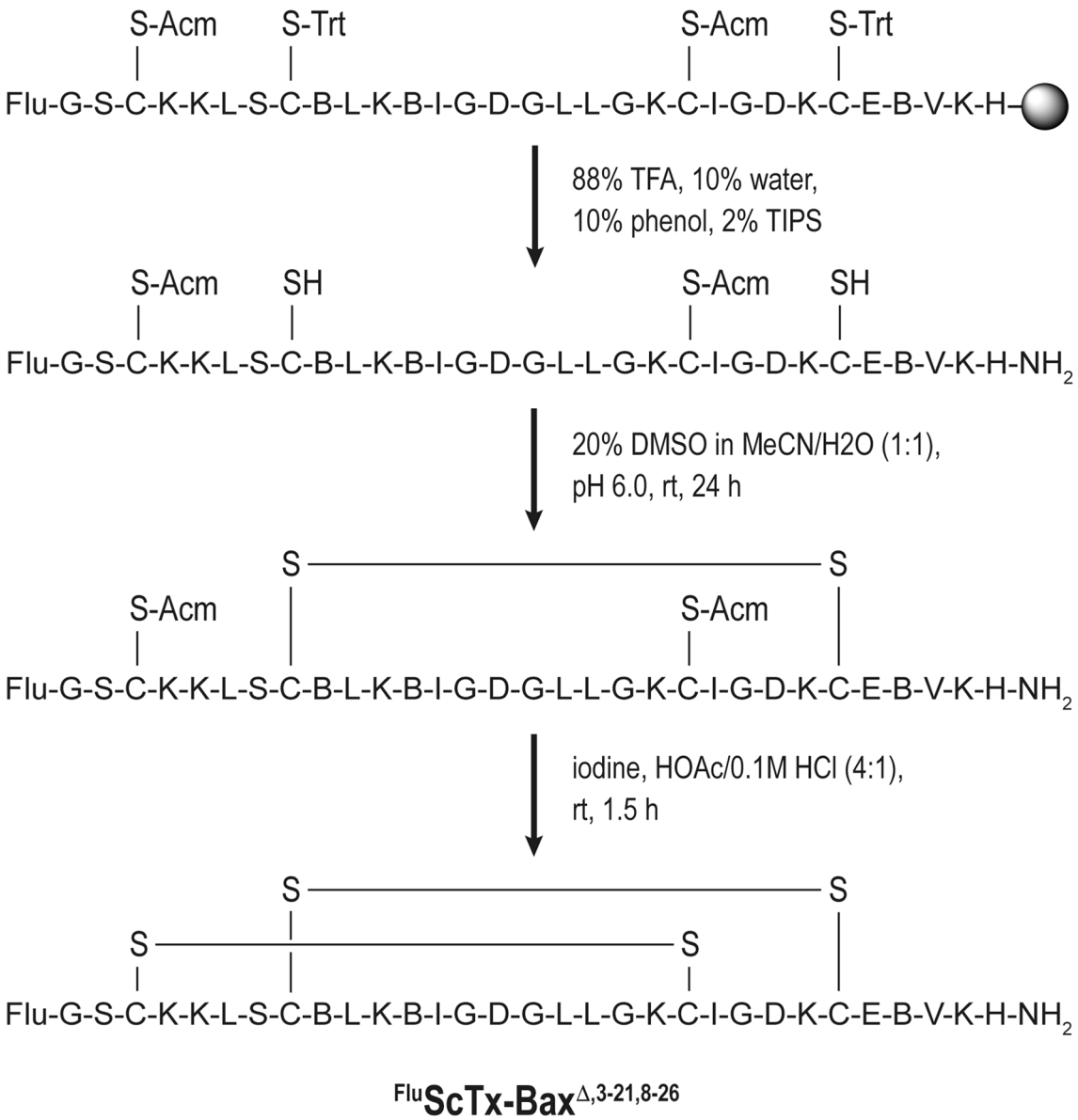

Fig. 2 Representative reaction scheme for the total chemical synthesis of ^{Flu}ScTx-Bax$^{\Delta}$ proteins using orthogonal protecting groups. Top sequence shows resin-bound peptide with S-Trt and S-Acm protected cysteine thiols. Reaction with aqueous TFA cleaves the peptide from the resin and removes all acid-labile protecting groups. Selective disulfide formation using DMSO in aqueous acetonitrile generates the semi-oxidized species. Subsequent deprotection of S-Acm with iodine in acetic acid, followed by concomitant disulfide formation, yields the fully-oxidized protein product

Thus, we speculate that the relatively large Acm protecting groups perturb the formation of disulfide linkages between thiols that lie adjacent to or near the protected cysteines. On the other hand, the higher conversion percentage seen with ^{Flu}ScTx-Bax$^{\Delta,3(Acm),21(Acm),8-26}$ may result from the flexibility of the N-terminal region of the peptide. We suggest that the steric bulk of the Acm groups within these constructs would be less of a hindrance to disulfides forming between residues C8–C26 within the peptide sequence. Despite modest-to-good yields for this initial oxidation, it was observed that these reactions were relatively clean, with no incidences of polymerization or formation of intermolecular disulfide bonds (Fig. 3a).

The second round of oxidation was performed *via* simultaneous deprotection and oxidation of the remaining cysteines contained within the ^{Flu}ScTx-Bax$^{\Delta}$ sequence. This was achieved by suspending the semi-oxidized products at a final concentration of 0.1 mg mL^{-1} in 0.05 M iodine in acetic acid/0.1 M HCl (4:1) and incubating the reaction mixture at room temperature for 1.5 h in the dark (Fig. 2). Following the

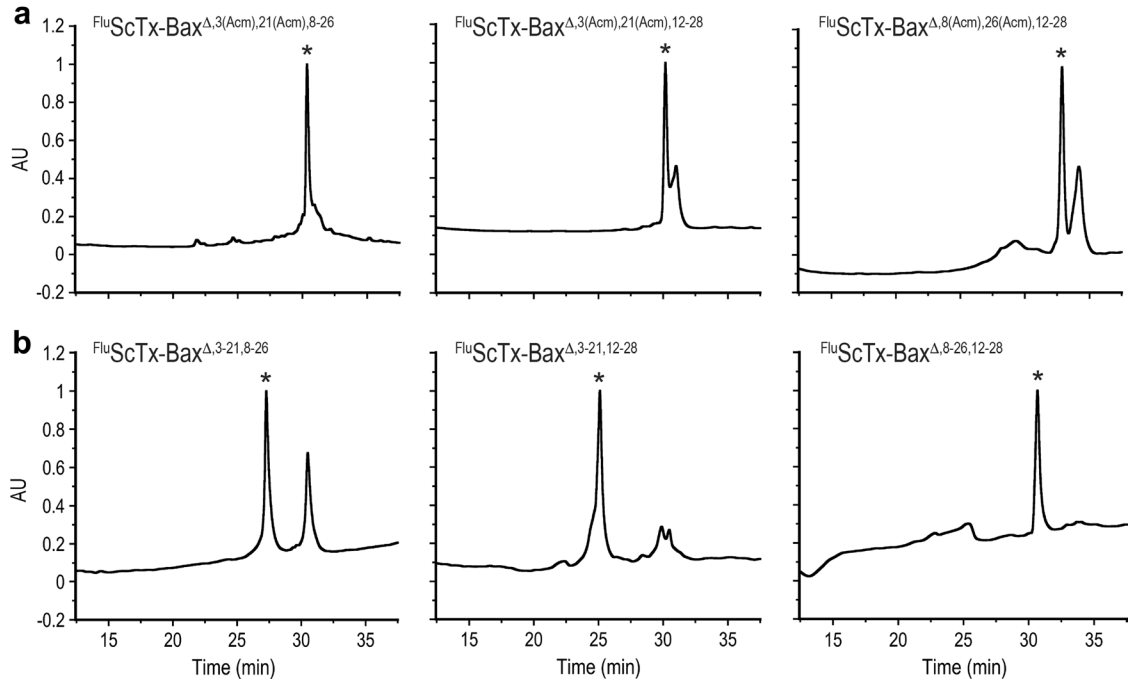

Fig. 3 Preparatory RP-HPLC chromatograms of semi- and fully-oxidized ^{Flu}ScTx-Bax$^{\Delta}$ proteins containing one or two disulfide linkages. **a** Spectra represent crude HPLC chromatograms of semi-oxidized peptides following oxidation with 20% DMSO in acetonitrile. Peaks marked with an asterisk (*) are those of fluorescently-labeled, semi-oxidized product. Peaks to the right of the product peaks are those of unreacted (reduced) starting material. **b** Spectra represent crude HPLC chromatograms of fully-oxidized peptides following oxidation with iodine. Peaks marked with an asterisk (*) are those of fluorescently-labeled, fully-oxidized product. Unreacted (semi-oxidized) starting material can be seen to the right of product peaks. All spectra were monitored at 214 nm. *AU* normalized absorbance units. See "Materials and Methods" section of main text for gradient details

reaction, the fully-oxidized protein products were purified using semi-preparative HPLC (Fig. 3b). Notably, the second oxidation reaction showed an opposite trend in conversion percentages compared to the initial DMSO-mediated oxidation. Forming the second disulfide in ^{Flu}ScTx-Bax$^{\Delta,3-21,8-26}$ proved the most difficult under these conditions, resulting in a 63.1% conversion to fully-oxidized product from the semi-oxidized starting material. ^{Flu}ScTx-Bax$^{\Delta,3-21,12-28}$ and ^{Flu}ScTx-Bax$^{\Delta,8-26,12-28}$ showed respective conversions of 74.2% and 97.6% to fully-oxidized products, indicating that the C12–C28 disulfide linkage may be influential in facilitating the formation of the second disulfide bond during these folding reactions. Moderately lower conversion percentages were seen in ^{Flu}ScTx-Bax$^{\Delta}$ variants containing disulfides between C3 and C21, indicating that this region of the peptide may be more flexible in solution, thus precluding efficient disulfide bond formation. It should again be noted that despite only modest-to-good overall conversion percentages for the fully oxidized proteins, each respective oxidation reaction produced a single, well-defined product peak by HPLC that was easily purified from the starting material (Fig. 3b). These results also indicated that no multimeric products or intermolecular disulfide linkages were formed over the course of the second oxidation. Once identified, all fully-oxidized protein products were purified to > 95% purity as determined by product peak integration of analytical HPLC chromatograms (Fig. S1).

3.3 Mapping and Assignment of Disulfide Bonds

Following synthesis and purification, the cysteine parings of each oxidized ^{Flu}ScTx-Bax$^{\Delta}$ variant were confirmed by mass analysis of trypsin-digested products. Proteolytic digestions were performed as described in "Materials and Methods" section. Briefly, fully-oxidized ^{Flu}ScTx-Bax$^{\Delta}$ proteins were treated with trypsin at 37 °C for 2 h in digestion buffer. Following incubation, the proteolysis reaction was terminated with the addition of 50% aqueous TFA. This procedure allowed for a high level of temporal control over the reaction, thus avoiding possible disulfide exchange that may occur in the produced fragments during longer proteolysis times [37]. Once the reaction was terminated, the product fragments were purified by HPLC and analyzed by electrospray ionization mass spectrometry (Table 1). This analysis demonstrated that each ^{Flu}ScTx-Bax$^{\Delta}$ construct contained two native disulfide bonds: C3–C21 and C8–C26 for ^{Flu}ScTx-Bax$^{\Delta,3-21,8-26}$; C3–C21 and C12–C28 for ^{Flu}ScTx-Bax$^{\Delta,3-21,12-28}$; and C8–C26 and

Table 1 Characterization of peptide fragments isolated from trypsin digests

BH3 domain mimetic	Peak retention time (min)[a]	Observed mass (Da)	Fragment sequence[b]	Identified cysteine pairs
^{Flu}ScTx-Bax$^{\Delta,3-21,8-26}$	23.74	1336.73	5–11; 26–30	C8–C26
	27.05	857.51	12–20	
	27.29	1284.50	1–4; 21–25	C3–C21
^{Flu}ScTx-Bax$^{\Delta,3-21,12-28}$	23.20	630.42	6–11	
	27.02	1284.46	1–4; 21–25	C3–C21
	28.00	1435.73	12–20; 26–30	C12–C28
^{Flu}ScTx-Bax$^{\Delta,8-26,12-28}$	16.69	2227.60	6–11; 26–30; 12–20	C8–C26; C12–C28
	20.20	516.98	21–25	
	25.45	734.27	1–4	

[a]Time observed from RP-HPLC chromatograms of trypsin digest fragments

[b]Numbers correspond to amino acid position in primary sequence

C12–C28 for ^{Flu}ScTx-Bax$^{\Delta,8-26,12-28}$. Mass spectra of peptide fragments isolated from trypsin digests are shown in Fig. S2.

3.4 Structural Characterization

The synthetic scheme in Fig. 2 outlines the total chemical synthesis of ^{Flu}ScTx-Bax$^{\Delta}$ proteins that contain two disulfide linkages at varying positions within the anticipated folded structure (Fig. 4a). For each individual construct, the disulfide linkages were either positioned near the N-terminus of the BH3 domain (^{Flu}ScTx-Bax$^{\Delta,3-21,8-26}$), at either ends of the BH3 domain (^{Flu}ScTx-Bax$^{\Delta,3-21,12-28}$), or near the C-terminus of the BH3 domain (^{Flu}ScTx-Bax$^{\Delta,8-26,12-28}$). Wild-type ScTx contains three disulfide bonds within its overall structural fold, however, it has been reported previously that just two disulfides are sufficient to fold ScTx proteins into structures that retain native and bio-active conformations [37]. Therefore, we speculated that two disulfide linkages would be sufficient for folding ScTx-Bax proteins into stable α/β structural motifs. The folding propensities of ^{Flu}ScTx-Bax$^{\Delta}$ proteins were evaluated using wavelength-dependent

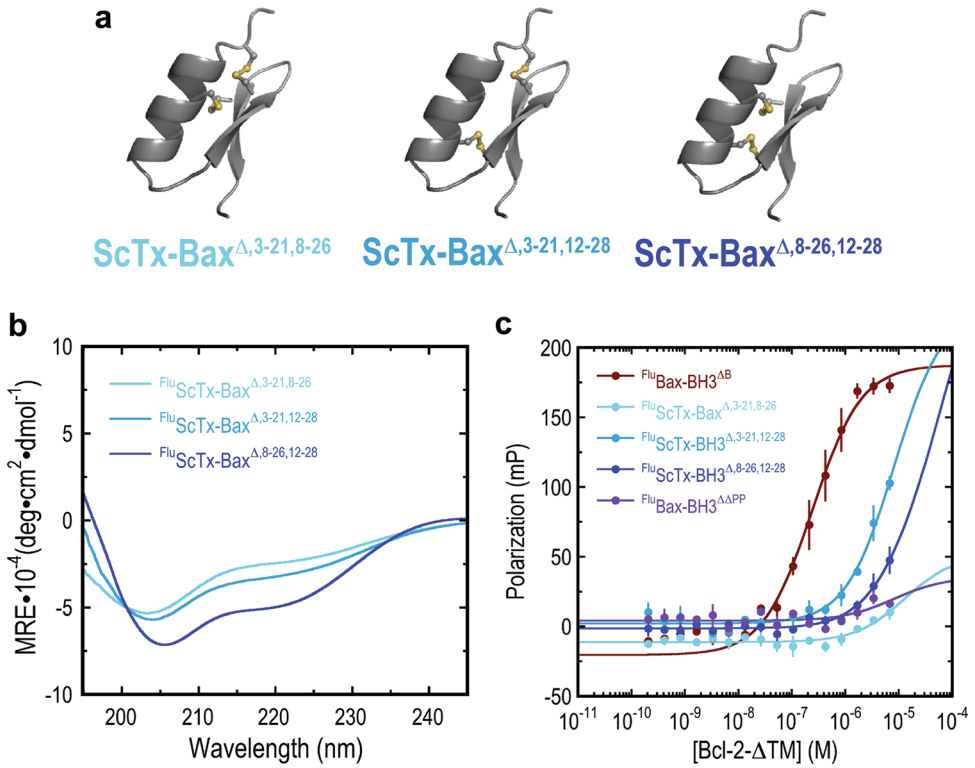

Fig. 4 **a** Three-dimensional models of folded ScTx-Bax domain mimetics showing the respective positions of disulfide linkages. Disulfide bonds are represented as ball and stick. **b** CD spectra of ^{Flu}ScTx-Bax$^{\Delta}$ peptides developed in this work. All peptides were dissolved at 5 μM in binding buffer for CD measurements at 20 °C. **c** Results from fluorescence polarization direct binding experiments of ^{Flu}ScTx-Bax$^{\Delta}$ variants targeting Bcl-2-ΔTM proteins in vitro. Data is representative of three separate experiments; error bars are standard deviation

CD spectroscopy (Fig. 4b). For these studies, all peptides were dissolved at a final concentration of 5 μM in binding buffer (50 mM Tris, 100 mM NaCl, pH 7.4) and CD spectra were collected at 20 °C. Under these conditions, all three ^{Flu}ScTx-Bax$^{\Delta}$ proteins displayed similar folds, with a minimum near 205 nm and a shoulder at 220 nm. Notably, the CD spectra exhibited by ^{Flu}ScTx-Bax$^{\Delta}$ proteins were comparatively similar to those of wild-type ScTx [29, 37], indicating the presence of an α/β structural conformation. It should be noted that both ^{Flu}ScTx-Bax$^{\Delta,3-21,8-26}$ and ^{Flu}ScTx-Bax$^{\Delta,3-21,12-28}$ showed modestly diminished CD signals compared to ^{Flu}ScTx-Bax$^{\Delta,8-26,12-28}$. These results suggest that the helical propensity for ScTx-Bax proteins is enhanced when covalent linkages are placed towards the C-terminal end of the helical BH3 domain and that disulfides placed towards the N-terminus of the helix result in a greater proportion of disordered conformation.

3.5 Targeting Anti-apoptotic Bcl-2 Proteins

The biological activity of ^{Flu}ScTx-Bax$^{\Delta}$ proteins was evaluated by testing their ability to target anti-apoptotic BCL2 proteins in vitro using direct FP binding assays (Fig. 4c). For these studies, recombinant His-tagged Bcl-2 proteins were expressed and purified from chemically competent BL21(DE3) bacteria cells using methods described previously [27, 33] (see "Materials and Methods" section). To facilitate purification and mitigate aggregation, Bcl-2 was expressed without its transmembrane domain (Bcl-2-ΔTM) [44]. BH3 domain mimetics ^{Flu}Bax-BH3$^{\Delta B}$ and ^{Flu}Bax-BH3$^{\Delta\Delta PP}$ were included in all FP direct binding assays as respective positive and negative controls. As expected, ^{Flu}Bax-BH3$^{\Delta B}$ targeted Bcl-2-ΔTM with high affinity, displaying a *Kd* of 208 nM (Table 2). The negative control peptide, ^{Flu}Bax-BH3$^{\Delta\Delta PP}$, which has been shown previously to display limited helical propensity [28], did not bind Bcl-2-ΔTM under these conditions. Similar FP assays using ^{Flu}ScTx-Bax$^{\Delta}$ proteins indicated that each variant bound Bcl-2-ΔTM with significantly different affinity, suggesting that the placement of the two disulfide linkages influences the ability for these constructs to target Bcl-2 in vitro (Fig. 4c; Table 2). Results from these assays showed that ^{Flu}ScTx-Bax$^{\Delta,3-21,8-26}$ was unable to bind Bcl-2-ΔTM under these conditions, indicating that positioning the disulfides near the N-terminus of the helix negatively affects favorable ScTx-Bax:Bcl-2 interactions. Alternatively, ^{Flu}ScTx-Bax$^{\Delta,3-21,12-28}$ and ^{Flu}ScTx-Bax$^{\Delta,8-26,12-28}$ bound Bcl-2-ΔTM with respective *Kd*s of 9.51 μM and 63.28 μM (Table 2). These results suggest that positioning the covalent linkages near the C-terminus or at opposite ends of the BH3 domain facilitates moderate binding to Bcl-2-ΔTM in vitro by ^{Flu}ScTx-Bax$^{\Delta}$ proteins. Despite only modest binding, these data collectively suggest that ScTx-based Bax-BH3 domain mimetics containing two disulfide linkages can be developed to target anti-apoptotic Bcl-2 proteins in vitro. Furthermore, these results indicate that placing two covalent linkages near the N-terminus of the Bax-BH3 domain abolish binding, while placing covalent linkages near the C-terminus or at either ends of the BH3 domain allow for moderately favorable ScTx-Bax:Bcl-2 interactions. We therefore speculate that BCL2:BH3 interactions are facilitated when there is some degree of flexibility at the N-terminus or within the central region of the BH3 domain.

Table 2 Data from direct in vitro binding experiments

BH3 domain mimetic	*Kd* (μM)
^{Flu}Bax-BH3$^{\Delta B}$	0.208
^{Flu}Bax-BH3$^{\Delta\Delta PP}$	ND
^{Flu}ScTx-Bax$^{\Delta,3-21,8-26}$	ND
^{Flu}ScTx-Bax$^{\Delta,3-21,12-28}$	9.51
^{Flu}ScTx-Bax$^{\Delta,8-26,12-28}$	63.28

ND not determined

3.6 Modeling the ScTx-Bax:Bcl-2 Interaction

In order to gain insight into the nature of the ScTx-Bax:Bcl-2 interaction, we employed PyMOL molecular modeling software [45] to align and dock ScTx-Bax proteins to the canonical BH3-binding groove of Bcl-2 (Fig. 5). The ScTx-Bax proteins developed in this work were designed to mimic the N-terminal region (residues 55–68) of the Bax-BH3 domain (Figs. 1b, 5a), with a total sequence identity of 76% across 17 residues. Structural alignment between the α-helix of ScTx-Bax (residues 5–15) and the N-terminus of the Bax BH3 domain (residues 58–68) showed that these regions overlay with an RMSD of 0.496 across 52 atoms (Fig. 5b). Notably, this structural model indicates that the α-helix of ScTx-Bax aligns well with the N-terminal region of the Bax-BH3 domain, while the β-sheet of ScTx-Bax points away from the ScTx-Bax:Bcl-2 binding interface. No steric clash was observed between the solvent-accessible surfaces of the two proteins. This model was further used to explore which residues within the ScTx-Bax protein interact with the BH3-binding groove of Bcl-2 (Fig. 5c, d). The putative BH3-binding epitope consists primarily of hydrophobic residues, including residues L59, L63, I66 and L70 of the Bax BH3 domain, and are highly conserved among pro-apoptotic BCL2 family members [46]. Essentially, these residues form a hydrophobic face on the BH3 α-helix that is capable of interacting with solvent-exposed hydrophobic sidechains within the BH3-binding groove of anti-apoptotic BCL2 proteins. More recently, crystallographic evidence has revealed that helical BH3 domains of pro-apoptotic BCL2 proteins also contain a relatively well-conserved sequence

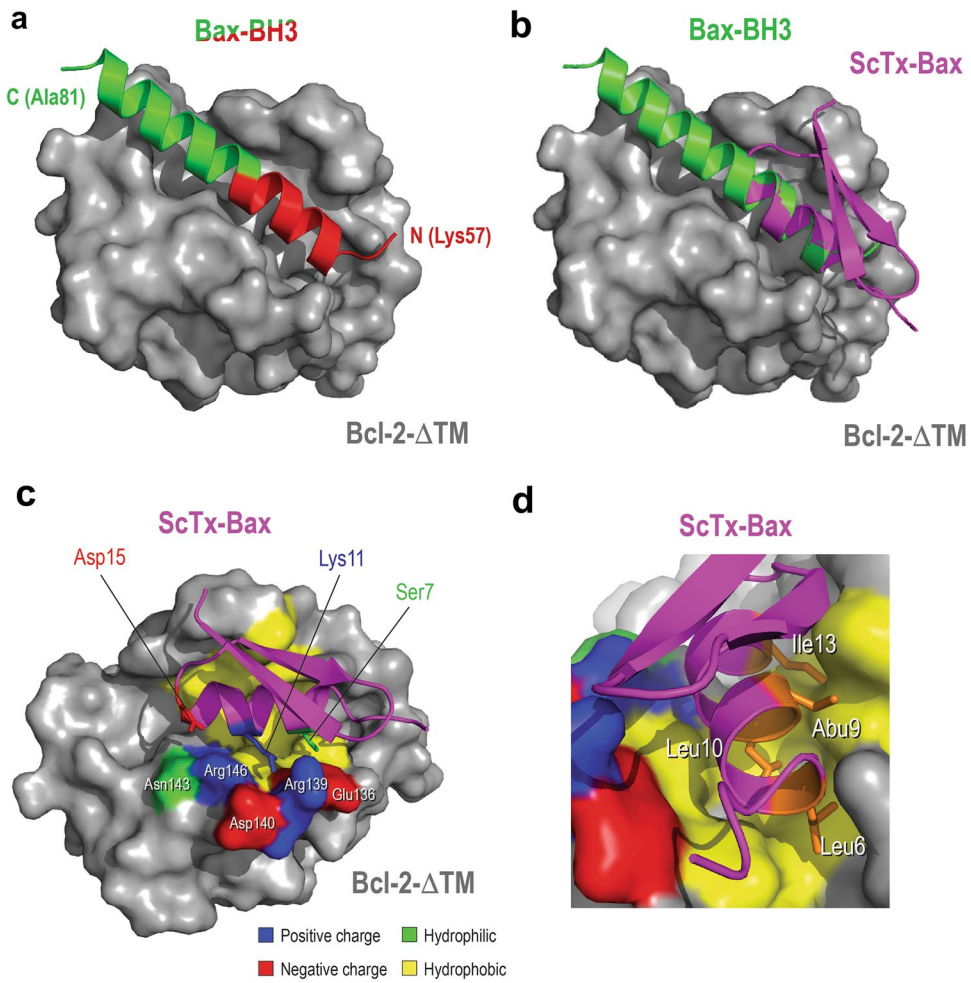

Fig. 5 Modeling the ScTx-Bax:Bcl-2 interaction. **a** Crystal structure of the Bax BH3 domain in complex with Bcl-2 (PDB ID: 2XA0). N-terminal region of the Bax BH3 domain helix that is mimicked by ScTx-Bax proteins is shown in red. **b** Structural alignment of ScTx-Bax with the Bax-BH3 domain in complex with Bcl-2. Residues 5–15 of the ScTx-Bax α-helix were aligned with residues 58–68 of the Bax-BH3 domain (RMSD = 0.496; 52 atoms). **c** Predicted binding mode of ScTx-Bax proteins within the canonical BH3-binding groove of Bcl-2. Hydrophobic, hydrophilic, positively charged and negatively charged residues are colored yellow, green, blue and red respectively. **d** Core conserved hydrophobic BH3 residues of ScTx-Bax (orange) make direct contact with the hydrophobic binding surface of Bcl-2 (yellow). (Color figure online)

of polar and charged amino acids that form salt bridges and hydrophilic interactions with an intricate network of polar residues that line the outside of the BH3 binding groove of anti-apoptotic BCL2 proteins [35, 44]. Indeed, many of these hydrophilic interactions are critical for favorable BCL2:BH3 interactions. For example, a highly conserved aspartate residue (D68) within the Bax BH3 domain is able to form a salt bridge with R146 on Bcl-2 [47] and mutating this aspartate to alanine (D68A) has been shown to significantly reduce favorable Bax interactions with anti-apoptotic BCL2 proteins [48, 49]. It should be noted that the design of our ScTx-Bax BH3 domain mimetics included an aspartate (D15) that corresponds to D68 of the Bax BH3 domain. The D15 residue was judiciously placed at the C-terminal end of the ScTx-Bax α-helix where, according to our structural model, it is capable of forming a salt bridge with R146 on Bcl-2 (Fig. 5c). Furthermore, our model suggests that several other charged or hydrophilic residues of ScTx-Bax, including S7 and K11, are capable of interacting with polar sidechains that line the outside of the canonical BH3-binding groove of Bcl-2. Finally, we used this model to confirm that the hydrophobic sidechains L6, L10 and I13 of ScTx-Bax, which correspond to respective sidechains L59, L63 and I66 of the Bax BH3 domain, are able to interact with the hydrophobic surface of the BH3-binding groove (Fig. 5d). Here, it was observed that each of these residues are well-positioned to interact with the hydrophobic surface of the Bcl-2 protein. Furthermore, this model illustrates that the hydrophobic aminobutyric acid residue (B9) of ScTx-Bax is positioned near the hydrophobic surface of the Bcl-2 BH3-binding groove. While this residue is not thought to be directly involved with the ScTx-Bax:Bcl-2 binding interaction, it seems to fit appropriately into the hydrophobic binding modality and thus should not negatively impact favorable ScTx-Bax:Bcl-2 interactions.

4 Discussion

In this report, we outline the total chemical synthesis of ScTx-Bax BH3 domain mimetics containing two disulfide linkages and evaluate their ability to target anti-apoptotic BCL2 proteins in vitro. For these studies, we synthesized a small library of fluorescently-labeled ScTx-Bax analogs:

^{Flu}ScTx-Bax$^{\Delta,3-21,8-26}$, ^{Flu}ScTx-Bax$^{\Delta,3-21,12-28}$, and ^{Flu}ScTx-Bax$^{\Delta,8-26,12-28}$ that each contained two native disulfide linkages at varying positions within the ScTx-Bax scaffold. Unfortunately, all attempts to simultaneously form both disulfide linkages using glutathione or platinum-based catalysts failed, resulting in heterogeneous mixtures of products containing non-native disulfide bonds. This prompted us to perform each oxidation reaction separately to ensure the proper patterning of disulfide linkages within the final product. By employing orthogonal Acm protecting groups on two cysteines and acid-labile Trt protecting groups on the other two cysteines within the primary sequence, we were able to perform sequential oxidation reactions that resulted in proper positioning of native disulfide linkages. Acid-mediated cleavage of the Acm-protected peptide from the resin afforded two exposed thiols that could effectively be oxidized by treatment with DMSO over 24 h. These reactions were relatively clean, with an average of 61.5% oxidation between all three species. Notably, the position of the Acm protecting groups significantly influenced the initial oxidation reaction, with ^{Flu}ScTx-Bax$^{\Delta,8(Acm),26(Acm),12-28}$ peptides showing the lowest conversion percentage (45.5%) and ^{Flu}ScTx-Bax$^{\Delta,3(Acm),21(Acm),8-26}$ giving the highest conversion percentage (78.3%). We therefore suggest that the relatively bulky Acm protecting groups influence the formation of disulfide linkages between thiols that lie adjacent to or near the protected cysteines. Subsequent removal of the Acm protecting groups, coupled with concomitant oxidation of the second disulfide resulted in the formation of ScTx-Bax variants containing two native disulfide linkages. It should be noted that yields for the second oxidation reaction also varied among the different ^{Flu}ScTx-Bax$^{\Delta}$ variants, with ^{Flu}ScTx-Bax$^{\Delta,8-26,12-28}$ resulting in the highest conversion (97.6%) and ^{Flu}ScTx-Bax$^{\Delta,3-21,8-26}$ having the lowest (63.1%) conversion among the three constructs. Because the disulfides closest to the C-terminus of the peptide were formed first, we attribute this drop in yield to the inherent flexibility of the N-terminus of the semi-oxidized peptide. Indeed, ^{Flu}ScTx-Bax$^{\Delta,3-21,8-26}$ is the only ^{Flu}ScTx-Bax$^{\Delta}$ construct that does not contain a C12–C28 linkage and this finding emphasizes the importance of this covalent bond in forming a second disulfide linkage within the context of ^{Flu}ScTx-Bax$^{\Delta}$ proteins.

Structural analysis of ^{Flu}ScTx-Bax$^{\Delta,3-21,8-26}$, ^{Flu}ScTx-Bax$^{\Delta,3-21,12-28}$, and ^{Flu}ScTx-Bax$^{\Delta,8-26,12-28}$ by wavelength-dependent CD spectrometry indicated that all three variants fold into stable α/β structural motifs reminiscent of wild-type ScTx [29, 37]. However, it was determined from these studies that the positioning of the disulfides had a modest impact on the solution-phase structure. For example, ^{Flu}ScTx-Bax$^{\Delta,8-26,12-28}$, where both disulfide linkages are positioned near the C-terminus of the helix, gave the most pronounced CD spectra of all variants tested under these conditions. On the other hand, ^{Flu}ScTx-Bax$^{\Delta,3-21,8-26}$ and ^{Flu}ScTx-Bax$^{\Delta,3-21,12-28}$, where the respective disulfides are positioned towards the N-terminus or on opposite ends of the BH3 domain, showed moderately diminished CD signals. These results suggest that the C3–C21 disulfide bond may have a slightly destabilizing effect on the solution-phase structure of ^{Flu}ScTx-Bax$^{\Delta}$ proteins.

The biological activity of ScTx-Bax$^{\Delta}$ proteins was evaluated by studying their ability to directly bind anti-apoptotic BCL2 proteins in vitro. Results from these studies indicated that ^{Flu}ScTx-Bax$^{\Delta,3-21,12-28}$ bound Bcl-2 with the highest affinity ($Kd = 9.51$ μM) compared to the other two sequence variants. ^{Flu}ScTx-Bax$^{\Delta,8-26,12-28}$ displayed the next highest affinity with a Kd of 63.28 μM, while an effective Kd was unable to be determined for ^{Flu}ScTx-Bax$^{\Delta,3-21,8-26}$. These results strongly suggest that the position of the disulfide linkages affects the ability for ^{Flu}ScTx-Bax$^{\Delta}$ proteins to bind Bcl-2 in vitro. Notably, positioning both disulfide linkages near the N-terminus of the helical BH3 domain, as with ^{Flu}ScTx-Bax$^{\Delta,3-21,8-26}$, completely abolished binding. These results are consistent with our previous results showing that a single disulfide linkage near the N-terminus of the BH3 domain negatively impacts the ability for ScTx-Bax proteins to target Bcl-2 under similar conditions [28]. Alternatively, positioning the (bis)disulfide linkages near the C-terminus of the BH3 helix, as with ^{Flu}ScTx-Bax$^{\Delta,8-26,12-28}$, rescued moderate binding to Bcl-2 in vitro. Interestingly, the ^{Flu}ScTx-Bax$^{\Delta}$ variant that showed the highest affinity for Bcl-2 in these studies was ^{Flu}ScTx-Bax$^{\Delta,3-21,12-28}$. In this construct, the disulfide linkages are placed at opposite ends of the helix, which may allow for some flexibility within the middle segment of the BH3 domain. Flexibility within this region may be important for the induced-fit binding mechanism required for favorable BCL2:BH3 interactions. Work in our laboratory is currently focused on determining the energetics of binding and the importance of each respective residue in the ScTx-Bax BH3 domain on BCL2 recognition.

Finally, we employed molecular modeling software in an effort to better understand the nature of the ScTx-Bax:Bcl-2 interaction. It was seen from these studies that ScTx-Bax proteins are able to adopt similar binding configurations as helical Bax BH3 domains when complexed with Bcl-2, with conserved hydrophobic L6, L10 and I13 residues all making contact with the hydrophobic binding surface of the canonical BH3-binding groove. Furthermore, it was shown that residues S7, K11 and D15 are able to make contact with polar sidechains that line the side of the binding groove. Importantly, we observed that D15 (ScTx-Bax) comes within 4.2 Å of R146 (Bcl-2) and may be able to form a salt bridge at this site. Indeed, this highly conserved ion pair has been shown to be crucial for favorable interactions among myriad BCL2 family members [46, 47]. Despite being simulations, these alignment studies support the

notion that favorable BCL2:BH3 interactions are facilitated not just through hydrophobic contacts, but through a complex network of hydrophobic, hydrophilic and electrostatic interactions. Furthermore, these modeling studies indicate that judicious placement of complementary residues along the α-helix of ScTx allows ScTx-Bax proteins to adopt a similar binding configuration as the Bax BH3 domain when complexed with Bcl-2.

In summary, the studies outlined herein clearly show that ScTx-Bax proteins containing two disulfide linkages can be synthesized using SPPS methods and screened for biological activity. These results indicate that the total chemical synthesis of ^{Flu}ScTx-Bax$^{\Delta}$ proteins requires orthogonal protecting groups and two rounds of oxidation. Furthermore, it was shown that just two disulfide bonds are sufficient to fold ScTx-Bax BH3 domain mimetics into structures similar to wild-type ScTx. However, given the ability for these constructs to target Bcl-2 with only modest affinity, we speculate that the presence of two disulfide linkages makes the structures too rigid to target anti-apoptotic Bcl-2 proteins with high affinity. Nevertheless, the results outlined in this study provide a viable synthetic route to ScTx-based protein mimetics that contain two native disulfide bonds.

Perhaps more critically, this study complements previous reports outlining the synthesis of ScTx-Bax BH3 domain mimetics containing 0, 1 or 3 disulfide linkages [27, 28]. Indeed, it is now possible to synthesize ScTx-Bax proteins that contain all combinations of native disulfides. The comprehensive nature of these studies has allowed us to determine the optimized number and position of disulfide linkages for targeting Bcl-2 proteins with ScTx-Bax BH3 domain mimetics in vitro. For instance, our earlier results showed that ScTx-Bax proteins containing three disulfide linkages did not bind Bcl-2 in vitro, while ScTx-Bax proteins containing no disulfides bound Bcl-2 with nanomolar affinity [27] (Table 3). This result supports the postulation that BH3 domains are unstructured in isolation and only become helical upon binding to other BCL2 proteins [23, 50]. Thus, having a helix locked into place with three disulfide linkages may hinder the induced-fit binding mechanism required for favorable BCL2:BH3 interactions. On the other hand, having just one disulfide present in ScTx-Bax proteins seems to allow for somewhat favorable interactions with Bcl-2 [28] (Table 3). Interestingly, it was gleaned from these studies that positioning the disulfide near the N-terminus of the ScTx-Bax BH3 domain completely abolished binding, while placing the disulfide in the middle or near the C-terminus of the helix rescued the ability for ScTx-Bax proteins to target Bcl-2 in vitro with nanomolar affinity. Furthermore, these studies showed that the positioning a single disulfide linkage near the middle of the helix allowed the ScTx-Bax protein to adopt a fold that was similar to wild-type ScTx [28, 29, 37] (Table 3). Results from the current study has demonstrated that just two disulfides are sufficient to fold ScTx-Bax BH3 domain mimetics into native-like conformations (Fig. 4b). However, the modest binding to Bcl-2 indicates that this particular configuration of disulfide patterning results in ScTx-Bax proteins that may be too rigid to bind Bcl-2 effectively (Fig. 4c). Nevertheless, the successful synthesis of ScTx-based protein domain mimetics containing two disulfides now allows for the generation of ScTx-based proteins containing any pattern of native disulfide linkages. With this development, we anticipate that ScTx-based mimetics will serve as valuable new tools for studying biomolecular recognition, as varied disulfide patterning can be optimized to target diverse molecular interaction surfaces. Furthermore, these collective findings may facilitate the expansion of ScTx-based miniature proteins as effective chemical genetics agents or as promising leads to next-generation protein-based therapeutics.

Table 3 Summary of direct in vitro binding experiments and structural analysis of ScTx-Bax BH3 domain mimetics containing 0, 1, 2 or 3 disulfide linkages

BH3 domain mimetic	Disulfide bonds	*Kd* (μM)	Structure[c]
^{Flu}Bax-BH3$^{\Delta B}$	–	0.208	–
^{Flu}Bax-BH3$^{\Delta\Delta PP}$	–	ND	–
^{Flu}ScTx-BH3$^{\Delta\Delta\Delta}$	0	0.269[a]	Unstructured
^{Flu}ScTx-Bax$^{\Delta\Delta,3-21}$	1	ND[b]	Unstructured
^{Flu}ScTx-Bax$^{\Delta\Delta,8-26}$	1	0.378[b]	ScTx-like
^{Flu}ScTx-Bax$^{\Delta\Delta,12-28}$	1	0.277[b]	Unstructured
^{Flu}ScTx-Bax$^{\Delta,3-21,8-26}$	2	ND	ScTx-like
^{Flu}ScTx-Bax$^{\Delta,3-21,12-28}$	2	9.51	ScTx-like
^{Flu}ScTx-Bax$^{\Delta,8-26,12-28}$	2	63.28	ScTx-like
^{Flu}ScTx-Bax	3	ND[a]	ScTx-like

ND not determined

[a]Values from [27]

[b]Values from [28]

[c]Determined by CD spectroscopy

Acknowledgements This work was supported in part by the Department of Chemistry and Biochemistry, the Edison Biotechnology Institute, the College of Arts and Sciences and the Vice President for Research at Ohio University. Additional funding for this research came from the Ohio University Baker Fund (Proposal #16-12). The authors would like to thank Professors Andrew Tangonan, Marcia Kieliszewski and Michael Held II for technical support.

Compliance with Ethical Standards

Conflict of interest The authors declare that they have no conflict of interest.

Ethical Approval This article does not contain any studies with human participants or animals performed by any of the authors.

References

1. Chin JW, Schepartz A (2001) Design and evolution of a miniature Bcl-2 binding protein. Angew Chem Int Ed Engl 40:3806–3809
2. Kritzer JA, Zutshi R, Cheah M, Ran FA, Webman R, Wongjirad TM, Schepartz A (2006) Miniature protein inhibitors of the p53-hDM2 interaction. Chembiochem 7:29–31
3. Sciarretta KL, Gordon DJ, Meredith SC (2006) Peptide-based inhibitors of amyloid assembly. Methods Enzymol 413:273–312
4. Wojcik P, Berlicki L (2016) Peptide-based inhibitors of protein-protein interactions. Bioorg Med Chem Lett 26:707–713
5. Walensky LD, Kung AL, Escher I, Malia TJ, Barbuto S, Wright RD, Wagner G, Verdine GL, Korsmeyer SJ (2004) Activation of apoptosis in vivo by a hydrocarbon-stapled BH3 helix. Science 305:1466–1470
6. Li C, Liu M, Monbo J, Zou G, Li C, Yuan W, Zella D, Lu WY, Lu W (2008) Turning a scorpion toxin into an antitumor miniprotein. J Am Chem Soc 130:13546–13548
7. Henchey LK, Porter JR, Ghosh I, Arora PS (2010) High specificity in protein recognition by hydrogen-bond-surrogate alpha-helices: selective inhibition of the p53/MDM2 complex. Chembiochem 11:2104–2107
8. Rutledge SE, Volkman HM, Schepartz A (2003) Molecular recognition of protein surfaces: high affinity ligands for the CBP KIX domain. J Am Chem Soc 125:14336–14347
9. Bottger A, Bottger V, Sparks A, Liu WL, Howard SF, Lane DP (1997) Design of a synthetic Mdm2-binding mini protein that activates the p53 response in vivo. Curr Biol 7:860–869
10. McColl DJ, Honchell CD, Frankel AD (1999) Structure-based design of an RNA-binding zinc finger. Proc Natl Acad Sci USA 96:9521–9526
11. Vita C, Drakopoulou E, Vizzavona J, Rochette S, Martin L, Menez A, Roumestand C, Yang YS, Ylisastigui L, Benjouad A, Gluckman JC (1999) Rational engineering of a miniprotein that reproduces the core of the CD4 site interacting with HIV-1 envelope glycoprotein. Proc Natl Acad Sci USA 96:13091–13096
12. Silverman AP, Levin AM, Lahti JL, Cochran JR (2009) Engineered cystine-knot peptides that bind alpha(v)beta(3) integrin with antibody-like affinities. J Mol Biol 385:1064–1075
13. Gilchrist J, Olivera BM, Bosmans F (2014) Animal toxins influence voltage-gated sodium channel function. Handb Exp Pharmacol 221:203–229
14. Janumyan YM, Sansam CG, Chattopadhyay A, Cheng N, Soucie EL, Penn LZ, Andrews D, Knudson CM, Yang E (2003) Bcl-xL/Bcl-2 coordinately regulates apoptosis, cell cycle arrest and cell cycle entry. EMBO J 22:5459–5470
15. Ola MS, Nawaz M, Ahsan H (2011) Role of Bcl-2 family proteins and caspases in the regulation of apoptosis. Mol Cell Biochem 351:41–58
16. Kvansakul M, Hinds MG (2015) The Bcl-2 family: structures, interactions and targets for drug discovery. Apoptosis 20:136–150
17. Youle RJ, Strasser A (2008) The BCL-2 protein family: opposing activities that mediate cell death. Nat Rev Mol Cell Biol 9:47–59
18. Reed JC, Zha H, Aime-Sempe C, Takayama S, Wang HG (1996) Structure-function analysis of Bcl-2 family proteins. Regulators of programmed cell death. Adv Exp Med Biol 406:99–112
19. Chao DT, Korsmeyer SJ (1998) BCL-2 family: regulators of cell death. Annu Rev Immunol 16:395–419
20. van Delft MF, Huang DC (2006) How the Bcl-2 family of proteins interact to regulate apoptosis. Cell Res 16:203–213
21. Cory S, Huang DC, Adams JM (2003) The Bcl-2 family: roles in cell survival and oncogenesis. Oncogene 22:8590–8607
22. Merino D, Bouillet P (2009) The Bcl-2 family in autoimmune and degenerative disorders. Apoptosis 14:570–583
23. Chen L, Willis SN, Wei A, Smith BJ, Fletcher JI, Hinds MG, Colman PM, Day CL, Adams JM, Huang DC (2005) Differential targeting of prosurvival Bcl-2 proteins by their BH3-only ligands allows complementary apoptotic function. Mol Cell 17:393–403
24. Placzek WJ, Wei J, Kitada S, Zhai D, Reed JC, Pellecchia M (2010) A survey of the anti-apoptotic Bcl-2 subfamily expression in cancer types provides a platform to predict the efficacy of Bcl-2 antagonists in cancer therapy. Cell Death Dis 1:e40
25. Oltersdorf T, Elmore SW, Shoemaker AR, Armstrong RC, Augeri DJ, Belli BA, Bruncko M, Deckwerth TL, Dinges J, Hajduk PJ, Joseph MK, Kitada S, Korsmeyer SJ, Kunzer AR, Letai A, Li C, Mitten MJ, Nettesheim DG, Ng S, Nimmer PM, O'Connor JM, Oleksijew A, Petros AM, Reed JC, Shen W, Tahir SK, Thompson CB, Tomaselli KJ, Wang B, Wendt MD, Zhang H, Fesik SW, Rosenberg SH (2005) An inhibitor of Bcl-2 family proteins induces regression of solid tumours. Nature 435:677–681
26. Wang D, Liao W, Arora PS (2005) Enhanced metabolic stability and protein-binding properties of artificial alpha helices derived from a hydrogen-bond surrogate: application to Bcl-xL. Angew Chem Int Ed Engl 44:6525–6529
27. Harris MM, Coon Z, Alqaeisoom N, Swords B, Holub JM (2016) Targeting anti-apoptotic Bcl2 proteins with scyllatoxin-based BH3 domain mimetics. Org Biomol Chem 14:440–446
28. Arachchige D, Margaret Harris M, Coon Z, Carlsen J, Holub JM (2017) Role of single disulfide linkages in the folding and activity of scyllatoxin-based BH3 domain mimetics. J Pept Sci 23:367–373
29. Martins JC, Van de Ven FJ, Borremans FA (1995) Determination of the three-dimensional solution structure of scyllatoxin by 1H nuclear magnetic resonance. J Mol Biol 253:590–603
30. Fields GB, Noble RL (1990) Solid phase peptide synthesis utilizing 9-fluorenylmethoxycarbonyl amino acids. Int J Pept Protein Res 35:161–214
31. Palasek SA, Cox ZJ, Collins JM (2007) Limiting racemization and aspartimide formation in microwave-enhanced Fmoc solid phase peptide synthesis. J Pept Sci 13:143–148
32. Shen F, Zhang ZP, Li JB, Lin Y, Liu L (2011) Hydrazine-sensitive thiol protecting group for peptide and protein chemistry. Org Lett 13:568–571
33. Kim KM, Giedt CD, Basanez G, O'Neill JW, Hill JJ, Han YH, Tzung SP, Zimmerberg J, Hockenbery DM, Zhang KY (2001) Biophysical characterization of recombinant human Bcl-2 and its interactions with an inhibitory ligand, antimycin A. Biochemistry 40:4911–4922
34. Golemi-Kotra D, Mahaffy R, Footer MJ, Holtzman JH, Pollard TD, Theriot JA, Schepartz A (2004) High affinity, paralog-specific recognition of the Mena EVH1 domain by a miniature protein. J Am Chem Soc 126:4–5
35. Ku B, Liang C, Jung JU, Oh BH (2011) Evidence that inhibition of BAX activation by BCL-2 involves its tight and preferential interaction with the BH3 domain of BAX. Cell Res 21:627–641
36. Ramachandran GN, Ramakrishnan C, Sasisekharan V (1963) Stereochemistry of polypeptide chain configurations. J Mol Biol 7:95–99
37. Zhu Q, Liang S, Martin L, Gasparini S, Menez A, Vita C (2002) Role of disulfide bonds in folding and activity of leiurotoxin I: just two disulfides suffice. Biochemistry 41:11488–11494
38. Nie C, Tian C, Zhao L, Petit PX, Mehrpour M, Chen Q (2008) Cysteine 62 of Bax is critical for its conformational activation and its proapoptotic activity in response to H_2O_2-induced apoptosis. J Biol Chem 283:15359–15369
39. Alias M, Ayuso-Tejedor S, Fernandez-Recio J, Cativiela C, Sancho J (2010) Helix propensities of conformationally restricted amino acids. Non-natural substitutes for helix breaking proline and helix forming alanine. Org Biomol Chem 8:788–792

40. Shi T, Rabenstein DL (1999) Trans-dichlorotetracyanoplatinate(IV) as a reagent for the rapid and quantitative formation of intramolecular disulfide bonds in peptides. J Org Chem 64:4590–4595
41. Shi T, Rabenstein DL (2000) Discovery of a highly selective and efficient reagent for formation of intramolecular disulfide bonds in peptides. J Am Chem Soc 122:6809–6815
42. Veber DF, Milkowski JD, Varga SL, Denkewalter RG, Hirschmann R (1972) Acetamidomethyl. A novel thiol protecting group for cysteine. J Am Chem Soc 94:5456–5461
43. Lamthanh H, Virelizier H, Frayssinhes D (1995) Side reaction of S-to-N acetamidomethyl shift during disulfide bond formation by iodine oxidation of S-acetamidomethyl-cysteine in a glutamine-containing peptide. Pept Res 8:316–320
44. Stewart ML, Fire E, Keating AE, Walensky LD (2010) The MCL-1 BH3 helix is an exclusive MCL-1 inhibitor and apoptosis sensitizer. Nat Chem Biol 6:595–601
45. Delano WL (2002) The PyMOL molecular graphics system. Delano Scientific, San Carlos
46. Petros AM, Olejniczak ET, Fesik SW (2004) Structural biology of the Bcl-2 family of proteins. Biochim Biophys Acta 1644:83–94
47. Gurudutta GU, Verma YK, Singh VK, Gupta P, Raj HG, Sharma RK, Chandra R (2005) Structural conservation of residues in BH1 and BH2 domains of Bcl-2 family proteins. FEBS Lett 579:3503–3507
48. Zha H, Aime-Sempe C, Sato T, Reed JC (1996) Proapoptotic protein Bax heterodimerizes with Bcl-2 and homodimerizes with Bax via a novel domain (BH3) distinct from BH1 and BH2. J Biol Chem 271:7440–7444
49. Nouraini S, Six E, Matsuyama S, Krajewski S, Reed JC (2000) The putative pore-forming domain of Bax regulates mitochondrial localization and interaction with Bcl-X(L). Mol Cell Biol 20:1604–1615
50. Rogers JM, Steward A, Clarke J (2013) Folding and binding of an intrinsically disordered protein: fast, but not 'diffusion-limited'. J Am Chem Soc 135:1415–1422